DYNAMICS OF 28.5 GeV ELECTRON AND POSITRON BEAMS IN A METER-LONG PLASMA

P. Muggli[*1], M.J. Hogan[†], B.E. Blue[Δ], C.L. O'Connell[†], K.A. Marsh[Δ], D. Walz[†], R. Iverson[†], F.-J. Decker[†], P. Raimondi[†], C.E. Clayton[Δ], S. Wang[Δ], S. Lee[*], E.S. Dodd[Δ], C. Joshi[Δ], C. Huang[Δ], T.C. Katsouleas[*], W.B. Mori[Δ]

[*]*University of Southern California, Los Angeles, CA 90089, USA*
[†]*Stanford Linear Accelerator Center, Stanford, CA 94309, USA*
[Δ]*University of California, Los Angeles, CA 90095, USA*

Abstract

A plasma wakefield accelerator (PWFA) experiment is conducted at the Stanford Linear Accelerator Center. The experiment aims at studying the issues relevant to a meter-long plasma accelerator module in the context of an actual high-energy collider. The transverse dynamics issues include transport and focusing of the beam. The longitudinal dynamics issues are the loss and gain of energy by the beam particles. Other physical phenomena such as the emission of radiation by the beam particles along their betatron motion, the steering of the electron beam when crossing a plasma/gas boundary, the beam impact ionization of neutral gases, and the light emitted by the plasma are also studied. Some of the experimental results obtained with electrons or positrons are presented.

Introduction

Plasmas can sustain very large electric fields, and plasma accelerators could thus play an important role in future high-energy electron-positron colliders. In the plasma wakefield accelerator[1] (PWFA) a short relativistic particle bunch drives a large amplitude plasma wave or wake and thus creates the high frequency accelerating structure in the plasma. Electrons or positrons can be accelerated by the longitudinal component of the wake[2,3]. The transverse component focuses the particle bunch. The PWFA is transformer in which the energy is transferred from the particles in the front of a single bunch or of a driver bunch to the particles in the back of the same bunch or to a trailing witness bunch. There are four main experimental issues that have to be addressed to demonstrate the relevance of the PWFA to present and future high-energy colliders. First, the acceleration of particles in a high gradient (>1 GeV/m) in a meter-long module has to be demonstrated. The field structure of the PWFA is strongly affected by the actual driver beam parameters (non-round beam, tilted beam, etc.). Impact ionization of the plasma ions and remaining neutral particles could create an additional plasma density. The dynamics of the newly created electrons could interfere with the PWFA dynamics in a pre-formed plasma. Second, the stable propagation of the particle beam in a dense, meter-long plasma has to be demonstrated. The maximum plasma density and/or the length over which the particle bunch can propagate are limited by the hose instability[4]. Third, the dimensions of the PWFA accelerating structure are in general of the same order as those of the particle bunch, and emittance dilution could result from the longitudinal and transverse variations of the wake fields over the beam size. Fourth, the linear theory for the PWFA shows that the maximum accelerating gradient that a bunch of Gaussian length σ_z with N particles can drive scales as[2]: $W_{max} \propto (N/\sigma_z^2)$. The scaling shows that gradients in the hundreds of MeV/m range can be expected with present bunches with a length σ_z 0.7 mm, and N 2×10^{10} particles/bunch in a plasma with a density n_e 1.5×10^{14} cm^{-3}. However, very short bunches (σ_z 100 to 12 μm) that could lead to multi-GeV/m energy gains in a plasmas with densities in the 10^{16} to 10^{17} cm^{-3} range[5] will become available soon[6]. All these issues have to be addressed with electron and positron beams. The main technical issues of the PWFA are the creation of meter-long uniform plasmas with the

[1] Corresponding author: muggli@usc.edu

appropriate density, as well as the control of the particle beam entering and exiting the PWFA module. It is thus very important to study the transverse and longitudinal dynamics of electron and positron beams in a meter-long PWFA module.

A PWFA experiment is currently performed at the Stanford Linear Accelerator Center (SLAC)[7]. The 28.5 GeV particle bunches of the final focus test beam[8] (FFTB) line with σ_z 0.7 mm and $N=2\times10^{10}$ particle/bunch are sent in a ≈1.4 m long plasma with an electron density n_e in the 0-2×10^{14} cm^{-3} range. A schematic of the experiment is shown on Fig. 1, and typical beam and plasma parameters are shown in Table I. With these parameters the beam density n_b is larger than the plasma density ($n_b>n_e$) and the experiment is performed in the non linear regime of the PWFA. This regime is interesting because the accelerating gradient is larger than that predicted be the linear theory. Also, the head of an electron bunch expels all the plasma electrons from the bunch volume. In this blowout regime the core of the electron bunch propagates in a pure ion column. The plasma ions partially neutralize the electron bunch, and the radial focusing electric field is linear with radius: $E_r(r)=(n_e e/2\varepsilon_0)r$. The focusing strength $B_\theta/r=n_e e/2\varepsilon_0 c$ is in the 0-6 kTesla/m range in this experiment. The bunch is focused by a very strong, ideal, extended plasma lens free of geometrical aberrations. PWFA experiments with lower (MeV) energy electron beams are either performed[9] or planed[10].

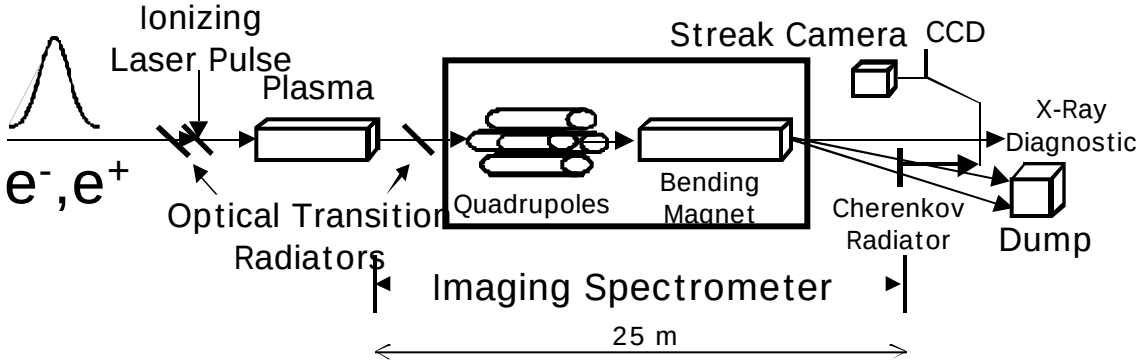

Figure 1: Schematic of the experiment with the imaging spectrometer (not to scale).

Parameter	Symbol	Value
Particles Energy	E	28.5 GeV
Beam Relativistic Factor	γ	55686
Number of e-, e+ per Bunch	N	2×10^{10}
Beam Energy		91 J
Bunch Length	σ_z	0.7 mm
Beam Power		40 TW
Bunch Radius @ Plasma Entrance	σ_x, σ_y	<40 μm
Beam Focused Intensity		8×10^{17} W/cm^2
Bunch Density	n_b	>10^{15} cm^{-3}
Normalized Beam Emittance	ε_{xN}	5×10^{-5} m-rad
	ε_{yN}	0.5×10^{-5} m-rad
Plasma Density	n_e	0-2×10^{14} cm^{-3}
Plasma Frequency		0-125 GHz
Plasma Length	L	1.4 m

Table I: Typical electron or positron beam, and plasma parameters. The beam parameters are before scattering through the various pellicles used in the experiment.

Experimental Set Up

The plasma is obtained by single-photon, laser photo-ionization of a lithium vapor produced in a heat-pipe oven [11]. The volume average plasma density at the time the laser is fired is obtained from the absorption of laser pulse uv photons and from the volume of the lithium vapor intercepted by the laser beam[12]. In the experiment the laser is typically fired a few μs prior to the particle

beam entering the plasma to allow for the plasma density to become more homogeneous by recombination and diffusion. The line integrated plasma density actually sampled by the particle beam is obtained from the particle beam parameters and from the variation of the beam spot size downstream from the plasma as a function of the laser pulse energy incident upon the lithium vapor. The plasma density at which the maximum accelerating gradient is produced given in the linear theory (n_b/n_e and $k_p\sigma_r<<1$) is such that $k_{pe}\sigma_z \sqrt{2}$, where k_{pe} is the plasma wave number: $k_{pe}=\omega_{pe}/c$, and $\omega_{pe}=(n_e e^2/\varepsilon_0 m_e)^{1/2}$ is the electron plasma frequency. It corresponds to $\approx 1.5\times10^{14}$ cm^{-3} for σ_z 0.7 mm. At this density the frequency of the accelerating wave is ≈110 GHz.

The particle beam spot size is monitored by imaging the optical transition radiation (OTR) emitted by the beam when traversing titanium foils (25 μm thick at 45°) located ≈1 m upstream from the plasma entrance and downstream from the plasma exit.

In early experiments the beam was allowed to travel ballistically from the plasma exit, through a dipole bending magnet, and through a thin piece of aerogel placed right after the magnet (≈12 m from the plasma exit), in which the particles emit Cherenkov radiation[13]. Imaging a fraction of the Cherenkov light onto a CCD camera yields the time integrated measurement of the beam spot size (σ_x, in the non-dispersive x-plane of the magnet) and of the beam energy (in the vertical y-plane). Imaging another fraction of the light onto the slit of streak camera yields a time-resolved measurement of the same quantities. For the latest rounds of experiments, quadrupoles were added between the plasma exit and the dipole magnet. They allow for the imaging of the particle beam at the plasma exit onto the piece of aerogel. The imaging property of the new spectrometer effectively eliminates the contribution to the energy measurement from the possible drift of the beam tail outside of the beam spot size. It also ensures that the vertical spread of the beam observed after the bending is a true representation of the particle beam energy content: $M_y\sigma_{y.\text{-}plasma\text{-}exit}<<\eta(\Delta E/E)$, where M_y 3 is the imaging magnification in the y-plane, η 10 cm is the magnetic dispersion at the aerogel location, and ΔE is the energy content of the particle beam. This was a very significant improvement of the experimental set up.

The incoming beam has a correlated energy spread of about 430 MeV, with the high energy particles in the head of the front, and the low energy particles in the back of the bunch (Fig. 2). Time integrated images of the beam after dispersion in energy, and thus to some extend in time, will therefore provide some insight into the beam transverse dynamics in the x-plane[14], as well as into the beam energy loss. The energy loss is experienced by the particles in the core and back of the bunch, already entering the plasma with a lower average energy (Fig, 2). However for the energy gain measurement both the imaging of the beam at the plasma exit and the time resolution will be necessary since the expected relative energy gain is of the same order as the incoming energy spread. Energy loss and gain results will be reported later.

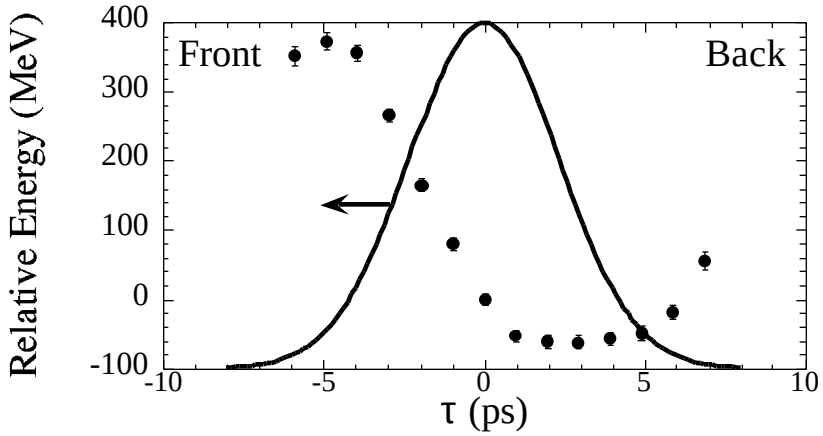

Figure 2: Measured correlated energy spread of the σ_z 0.7 mm incoming electron bunch, as obtained from the analysis of a streak camera images with ≈1 ps resolution. The bunch travels from right to left.

Electron Plasma Focusing

In the experiment the particle beam is focused near the plasma entrance (z=0). The beta function of the beam $\beta_{beam}=\gamma\sigma_{x,y}/\varepsilon_{N\,x,y}$ is shorter than the plasma length L, and the plasma acts on the beam as an extended plasma length. In the electron beam case in the blow out regime, the focusing strength of the plasma reaches its pure ion column value early in the bunch and more than 75% of

the beam particles experience that focusing strength[15]. The evolution of the electron beam spot can thus calculated using a beam envelope equation[16]:

$$\frac{d^2\sigma_{x,y}(z)}{dz^2} + \left[K^2 - \frac{\varepsilon_{Nx,y}^2}{\gamma^2\sigma_{x,y}^4(z)}\right]\sigma_{x,y}(z) = 0 \qquad (1)$$

in which the action of the plasma is described by the restoring constant $K=\omega_{pe}/(2\gamma)^{1/2}c$. In vacuum the beam size downstream from the plasma is $\sigma_{x,y}(z)= \sigma_{x,y}(0)[1+\varepsilon_{N\,x,y}{}^2z^2/\gamma^2\sigma_{x,y}{}^4(0)]^{1/2}$ (solution to Eq. 1 with n_e=0). In the plasma the beam envelope oscillates with a spatial period equal to half the betatron period of the particle $\lambda_\beta=2\pi/K=2\pi c(2\gamma)^{1/2}/\omega_{pe}$. The plasma density is assumed to be constant over the length of the plasma L. The beam and the plasma can be matched, and the beam envelope oscillation in the plasma suppressed, by choosing the experimental parameters such that the term in the brackets in Eq. 1 vanishes. The radius matched to a plasma with a density optimum for acceleration (n_e 1.5×10^{14} cm^{-3}) is ≈12 μm. Fig.3 b shows the beam as observed that the downstream OTR location (≈2.4 m from the plasma entrance) after propagation in vacuum (n_e=0) for the case of a size at the plasma entrance of $\sigma_x(0)$=14 μm ($\sigma_y(0)$=9 μm), normalized emittance after scattering of ε_{Nx}=18×10^{-5} m-rad (β_{x0}=6.1 cm) (ε_{Ny}=4×10^{-5} m-rad, β_{y0}=10.5 cm) and a waist located ≈4 cm (≈2 cm) before the plasma entrance in the x-plane (y-plane respectively). The spot sizes obtained from Gaussian fits to image summed in the x-, and y-directions are σ_x=575 μm and σ_y=155 μm. Figures b shows the beam observed at the same location this time in the case of n_e 1.3×10^{14} cm^{-3} over ≈1.4 m. At this plasma density the spot size is at a minimum in the x-plane, but not in the y-plane, because the beam parameters are different in both planes. The measured spot sizes are σ_x 110 μm and σ_y 70 μm. The beam spot size reduction in the x-plane at this location is thus larger than five. The beam propagation was stable up to a plasma density of ≈5×10^{14} cm^{-3}, and no significant hose instability was observed[17].

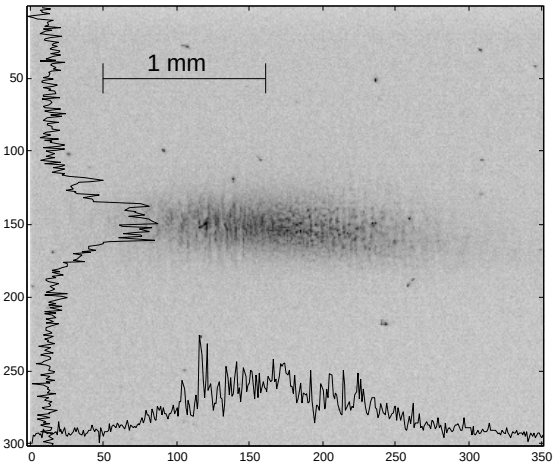

Figure 3a: Electron beam, n_e=0 cm^{-3}, unfocused, σ_x=575 μm, σ_x=155 μm. Also shown, line outs through the image peak.

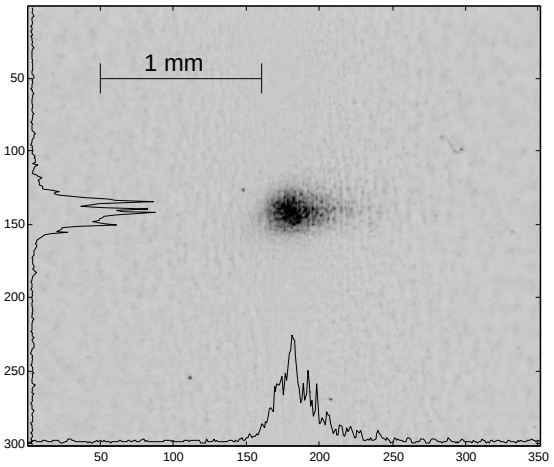

Figure 3b: Electron beam, n_e 1.3×10^{14} cm^{-3}, focused, σ_x=110 μm, σ_x=70 μm

Positron Plasma Focusing

A plasma can also focus a positron bunch. [18] In the case of positrons, the plasma electrons are attracted toward the positron bunch, and partially neutralize the space charge field of the positron bunch, which is focused. However, there is no blow out regime with positrons since plasma electrons will be attracted from a plasma skin depth away of the beam. Electrons from different radii reach the bunch volume at different times. The focusing process is thus very dynamic, with the focusing strength varying both along the beam, and in the transverse dimension. This leads to emittance dilution of the positron beam. At low plasma density, the positron beam can be partially neutralized, and overall focusing of the bunch can be expected. Figure 4a shows the positron beam at the downstream location for the case of an round beam radius of 25 μm, focused at the plasma entrance, without plasma (n_e=0). The emittance of the beam in both planes is similar to that of the electron beam. The beam spot sizes are σ_x=634 μm and σ_y=122 μm. Figure 4b shows the beam at the same location in the case of n_e 1.5×10^{14} cm^{-3} over ≈1.4 m.

The beam is focused in the x-plane to spot sizes of σ_x=344 μm and the Gaussian fit indicates that the beam is defocused in the y-plane toσ_y=243 μm. The images shows the presence of a particle halo around the focused core of the beam. The spot size is composed of a narrow part of the beam sitting on top of an unfocused shoulder and the Gaussian spot sizes are larger than expected from the image line outs shown on Fig. 4. The transverse dynamics induced by the plasma electrons rushing into the beam volume can be greatly reduced by propagating the positron beam in a hollow plasma channel[3]. The hollow channel also enhances the accelerating gradient by helping to synchronize the plasma electron rushing on axis, since they all originate from a radius larger than that of the hollow plasma channel. Partially hollow plasma channels with different radius have been produced by placing a mask in the ionizing laser beam path. The laser beam casts a shadow of into the lithium vapor, thereby creating the channel. The results obtained with the channel will be presented elsewhere.

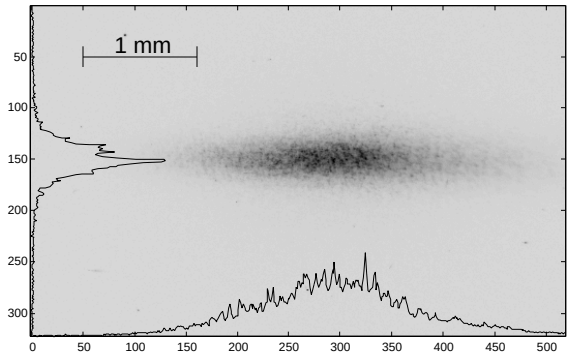

Figure 4a: Positron beam, n_e=0 cm^{-3}, unfocused, σ_x=634 μm, σ_x=132 μm. Also shown, line outs through the image peak.

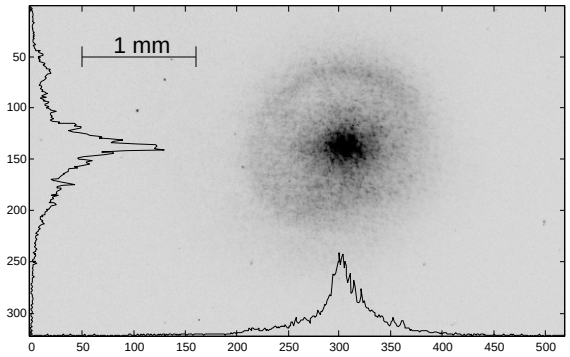

Figure 4b: Positron beam, n_e 1.5×10^{14} cm^{-3}, focused, σ_x=344 μm, σ_x=243 μm.

Betatron Radiation

The beam electrons are accelerated along their betatron motion in the plasma. As a result an electron starting at a radius r_0 oscillating at the betatron frequency $\omega_b=\omega_{pe}/\sqrt{(2\gamma)}$, emits radiation with a characteristic wavelength given by[19]:

$$\omega_r = 2m\gamma^2\omega_b \Big/ \left(1 + K_w^2/2 + (\gamma\Omega)^2\right)$$

where m=1,2,… is the harmonic number, $K=\gamma\omega_b r_0/c$ is the plasma wiggler strength, and Ω is the observation angle measured from the axis. Since there are electrons with all radii between *0* and $\sigma_{x,y}$, K_w varies continuously through the beam radius and reaches 15 (K_w>>1) at $\sigma_{x,y}$ 40 μm, and the radiation is emitted in a broadband spectrum. For the parameters of Table I, the spectrum cut-off frequency[20] $\omega_c=3\gamma c r_0\ \omega_b^2/2c$ is in the x-ray range, and is emitted in a very narrow angle θ K_w/γ, in the forward direction. This radiation was observed for photon with energies between 5 and 30 keV, using a silicon wafer as Bragg scatterer and reflector, and surface barrier detectors[21]. The peak spectral brightness at a photon energy was estimated to be ≈7×10^{18} photons/sec//mrad^2/mm^2/0.1%bandwidth. Plasmas could thus be used as simple wigglers to produce very high brightness, tunable radiation in the visible to x-ray wavelength range.

Collective Electron Beam Refraction

In a homogeneous plasma, the ion channel produced by a short cylindrical electron is also cylindrical with a radius r_c α$(N/(2\pi)^{3/2}\sigma_z n_e)^{1/2}$, where α 1 for a long bunch and α 2 for a short bunch of the order of a plasma wavelength long. The focusing is provided by the partial neutralization of the beam space charge, or equivalently by the focusing field of the ion column within the beam volume. In a plasma with a density gradient, the focusing force becomes asymmetric and the beam is steered by the plasma[22]. When the beam crosses the boundary between the plasma and the surrounding vacuum or neutral gas, the ion channel becomes asymmetric (positive charges missing on the vacuum side), and the beam is collectively deflected toward the plasma boundary. This collective deflection of the electron beam at the plasma/vacuum boundary can be seen as the analogous to

the refraction of a photon beam at a dielectric interface. It can be described by a non-linear Snell's law[23]. This effect has been measured for the first time, and was found to follow the expected angular dependency[24].

Impact Ionization

Lithium was chosen for plasma because of its low atomic number Z. The 28.5 GeV beam particle can create additional plasma density by direct impart ionization. More over, the cross section for impact ionization peaks at an energy of about 100 eV[25] and is about two orders of magnitude larger than around 28.5 GeV. Plasma electrons created by direct impact ionization could therefore create an even much larger additional plasma density in subsequent collisions. The dynamics of the electrons created by impact ionization could interfere with the formation of the accelerating gradient expected from the PWFA mechanism in a pre-formed plasma. To evaluate the amount of plasma created by the electron and positron beam in the experiment.[26], the Li vapor is replaced by neutral gases with various Z: He, Ar, Ne, and N_2. The beam spot size is then measured as a function of the gas pressure at different locations. Because of the additional time within the particle bunch necessary to create the plasma, the plasma density necessary for a spot size reduction (at a given location) is probably larger than for the same spot size reduction in the pre-formed plasma case. Experimental results show that for helium there is no noticeable spot size reduction in the pressure range typical of the oven operation (He with Z=2 pressure ≈0.4 Torr, Li with Z=3 and pressure of ≈0.1 T). This is confirmed by full tri-dimensional particle-in-cell simulations of the PWFA with the present experimental parameters[27]. However, plasma sources capable of producing plasma densities appropriate for PWFA experiments with much shorter bunch length[5] or future energy doubler systems[28], may use large Z atomic vapors such as rubidium, or cesium[29]. In principle higher Z vapors also require higher Z buffer gases at higher pressures. Strong focusing is observed in a few Torrs of Ar, Ne, or N_2. Impact ionization may thus become an issue in devices operating in this pressure range.

Summary

The dynamics of 28.5 GeV electron and positron beams in a 1.4 m long PWFA module has been studied in a regime where the beam density is larger than the plasma density. The plasma acts on the particle beam as an extended plasma lens, and both electron[15] and positron beams are focused. The propagation of the electron beam appears to be stable[17] up to densities relevant for plasma acceleration of the σ_z 0.7 mm beam: $n_e \approx 5\times10^{14}\text{cm}^{-3}$. The experimental set up has been modified to allow for the imaging of the beam at the plasma exit into the plane where the energy diagnostic is performed. Experimental results regarding the energy loss and gain by the beam particles will be reported in the near future. Other very interesting phenomena have been observed and studied: the collective refraction of the electron beam at the plasma/gas boundary[24], the wiggler action of the plasma on the electron beam leading to the emission of high brightness radiation in the x-ray energy range[21], and the focusing of both electron[26] and positron beams by the plasma density they create by impact ionization of noble various gases. Shorter electron bunches will be available very soon at the Stanford Linear Accelerator Center[6], and experiments will be performed with σ_z 100 μm electron bunches. Energy gains in excess of one GeV are expected over a plasma length ≈30 cm with a density in the $5\text{-}8\times10^{15}$ cm^{-3}. One can envisage that PWFA could be used in the near future to double the final energy of a linear electron-positron collider over a short distance[28].

Acknowledgements

Work supported by USDoE #DE-FG03-92ER40745, DE-AC03-76SF00515, #DE-FG03-98DP00211, #DE-FG03-92ER40727, NSF #ECS-9632735, NSF #DMS-9722121. We would like to thank Dr. Peter Tsou of JPL for providing the aerogel.

References

[1] T. Tajima and J.M. Dawson, phys. Rev. Lett. 43, 267 (1973), P. Chen *et al.*, Phys. Rev. Lett. 54, 693 (1985).

[2] P. Chen *et al.*, UCLA Report PPG-802 , (1984), P. Chen *et al.*, Phys. Rev. Lett. 54, 693 (1985), S. Lee *et al.*, Phys. Rev. E 61(**6**), 7014 (2000).

[3] S. Lee *et al.*, Phys. Rev. E 64, 045501 (2001).

[4] D.H. Whittum, Journal of Physics D 30(21), 2958 (1997).

[5] E-164 proposal, ARDB Technical note, ARDB260, SLAC, September 2001.

[6] P. Emma *et al.*, Poceedings PAC 2001 Conference, 4038 (2001).

[7] R. Assmann *et al.*, Nucl. Instr. Meth. Phys. Res. A 40(3), 396 (1997).

[8] V. Balakin *et al.*, Phys. Rev. Lett. 74, 2479 (1995).

[9] N. Barov *et al.*, PRST-AB 3(1), 011301 (2000).

[10] A.Ts. Amatuni *et al.*, Proceedings of the Part. Acc. Conference, New York NY, 3657 (1999), C.E. Clayton *et al.*, Proceedings of the Part. Acc. Conference, Vancouver Canada, 678 (1997)

[11] C.R. Vidal and J. Cooper, J. Appl. Phys. 40(**8**), 3370 (1960).

[12] P. Muggli *et al.*, IEEE Trans. On Plasma Science 27(**3**), 791 (1999).

[13] M.J. Hogan *et al.*, Phys. of Plasmas 7, 2241 (2000).

[14] C. L. O'Connell *et al.*, to be submitted to PRST-AB.

[15] C.E. Clayton *et al.*, accepted for publication in Phys. Rev. Lett. (2002).

[16] K.G. Steffen, in High Energy Beam Optics, Interscience: John Wiley, New York, 173 (1965).

[17] B. Blue *et al.*, to be submitted to Phys. Rev. Lett. (2002).

[18] J.S.T. Ng *et al.*, Phys. Rev. Lett. 87, 244801-1 (2001).

[19] E. Esarey *et al.*, AIP Proceedings, 569, 473, (2001).

[20] J. D. Jackson, Classical Electrodynamics ,J. Wiley and Sons, N.Y., 662 (1975).

[21] S. Wang *et al.*, to appear in Phys. Rev. Lett. (2002).

[22] W.B. Mori, *et al.*, Bull. Am. Phys. Soc. 46(8), 91 (2001).

[23] T.C. Katsouleas *et al.*, Nucl.Instr. Meth. Phys. Res. A 455, 161 (2000).

[24] P. Muggli *et al.*, Nature 411, 43 (2001), P. Muggli *et al.*, PRST-AB 4(9), 091301 (2001).

[25] S.M. Younger and T.D. Märk, in Electron Impact Ionization, Springer-Verlag, Vienna, 25 (1985).

[26] B. Blue *et al.*, Bull. Am. Phys. Soc. 46(8), 91 (2001).

[27] D. Bruhwiler *et al.*, PRST-AB 4(10), 101302 (2001).

[28] S. Lee *et al.*, PRST-AB 5, 011001 (2002).

[29] K.A. Marsh, private communication.